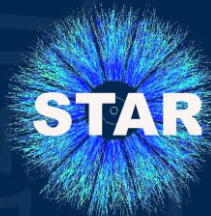


Partially funded by:



ELTE
EÖTVÖS LORÁND
UNIVERSITY

Two-particle interferometry with Lévy-stable sources in Au+Au collisions at **STAR**



Dániel Kincses for the STAR Collaboration
Eötvös University, Budapest

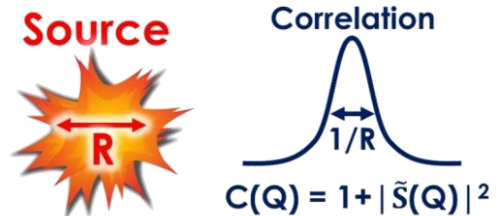
23rd ZIMÁNYI SCHOOL WINTER WORKSHOP
ON HEAVY ION PHYSICS, December 4-8, 2023,
BUDAPEST



Part I. Introduction, Motivation



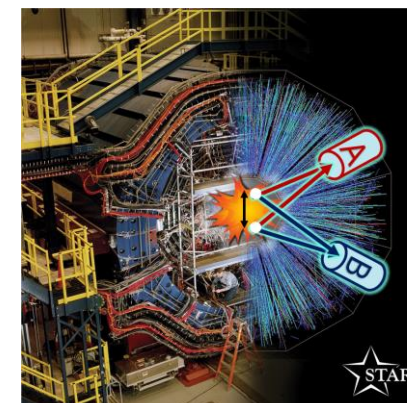
Basic definitions of femtoscopic correlation functions



- Single particle momentum distribution: $N_1(p) = \int d^4x S(x, p)$ phase-space density
- Pair momentum distribution: $N_2(p_1, p_2) = \int d^4x_1 d^4x_2 S(x_1, p_1) S(x_2, p_2) |\psi_{p_1, p_2}(x_1, x_2)|^2$
- Correlation function:
- Pair source/spatial correlation: $C(p_1, p_2) = \frac{N_2(p_1, p_2)}{N_1(p_1) N_1(p_2)}$ pair separation
- relative pair momentum average pair momentum*
- $C(Q, K) = \int d^4r D(r, K) |\psi_Q(r)|^2$ Pair wave function, containing FSI!
- *Instead of K , m_T is often used:
 $m_T = \sqrt{k_T^2 + m_\pi^2}$, $k_T = \sqrt{K_x^2 + K_y^2}$
- Experiments: measuring $C(Q) \rightarrow$ information about $D(r)$ and FSI
- Experimental (and phenomenological) indications:
power-law tail for pions, **non-Gaussianity?**

D. A. Brown and P. Danielewicz. In: Phys. Lett. B 398 (1997), pp. 252–258.

S. S. Adler et al., PHENIX Coll. In: Phys. Rev. Lett. 98 (2007), p. 132301.



$$S(\mathbf{r}) = \mathcal{L}(\alpha, R; \mathbf{r}) = \frac{1}{(2\pi)^3} \int d^3 q e^{i \mathbf{q} \cdot \mathbf{r}} e^{-\frac{1}{2} |\mathbf{q}^T \mathbf{R}^2 \mathbf{q}|^{\alpha/2}}$$

spherical sym.: $R_{ij}^2 = R^2 \delta_{ij}$

What is the shape of the source?

Gaussian vs. Lévy distributions in heavy-ion physics

Csörgő, Hegyi, Zajc, Eur.Phys.J.C 36 (2004) 67

- **Symmetric Lévy-stable distribution**

- From generalized central limit theorem, power-law tail (if $\alpha < 2$) $\sim r^{-(1+\alpha)}$
- $\alpha = 2$ Gaussian, $\alpha = 1$ Cauchy
- Retains the same α under convolution

$$S(r) = \mathcal{L}(\alpha, R; r)$$

$$D(r) = \mathcal{L}(\alpha, 2^{1/\alpha} R; r)$$

- **Experimental indications – Lévy source for pion pairs?**

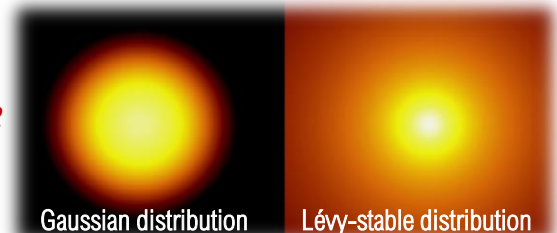
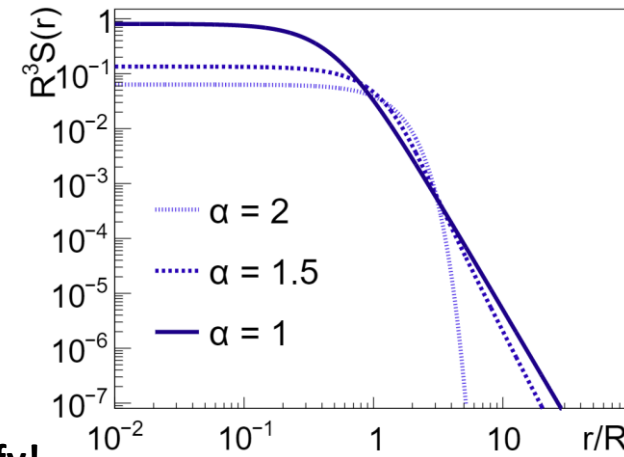
- **RHIC (PHENIX, STAR)** *Phys.Rev. C97 (2018) no.6, 064911*
- **LHC (CMS)** *Phys.Part.Nucl. 51 (2020) 3, 267-269*
arXiv:2306.11574 (CMS-HIN-21-011)
- **SPS (NA61/SHINE)** *Eur.Phys.J.C 83 (2023) 10, 919*

See talk of
M. Csanád
and B. Pórfy!

- **Possible interpretations of the α Lévy exponent based on:**

- Jet fragmentation *Csörgő, Hegyi, Novák, Zajc, Acta Phys.Polon. B36*
- Critical behavior *Csörgő, Hegyi, Novák, Zajc, AIP Conf.Proc. 828*
- Event averaging *Cimerman, Tomaszik, Plumberg, Phys.Part.Nucl. 51 (2020) 3, 282*
- Resonance decays *Kincses, Stefaniak, Csanád, Entropy 24 (2022) 3, 308*
- Anomalous diffusion *Csanád, Csörgő, Nagy, Braz.J.Phys. 37 (2007) 1002;*

- **Lévy in 1D: not because of 3D→1D conversion!** *Kurylis, Acta Phys. Pol. B Proc. Suppl. vol. 12 (2), 477 (2019)*



New data analyses and phenomenological investigations are needed to gain a better understanding!

$$S(\mathbf{r}) = \mathcal{L}(\alpha, R; \mathbf{r}) = \frac{1}{(2\pi)^3} \int d^3 q e^{iqr} e^{-\frac{1}{2}|\mathbf{q}^T \mathbf{R}^2 \mathbf{q}|^{\alpha/2}}$$

spherical sym.: $R_{ij}^2 = R^2 \delta_{ij}$

Lévy source at RHIC energies

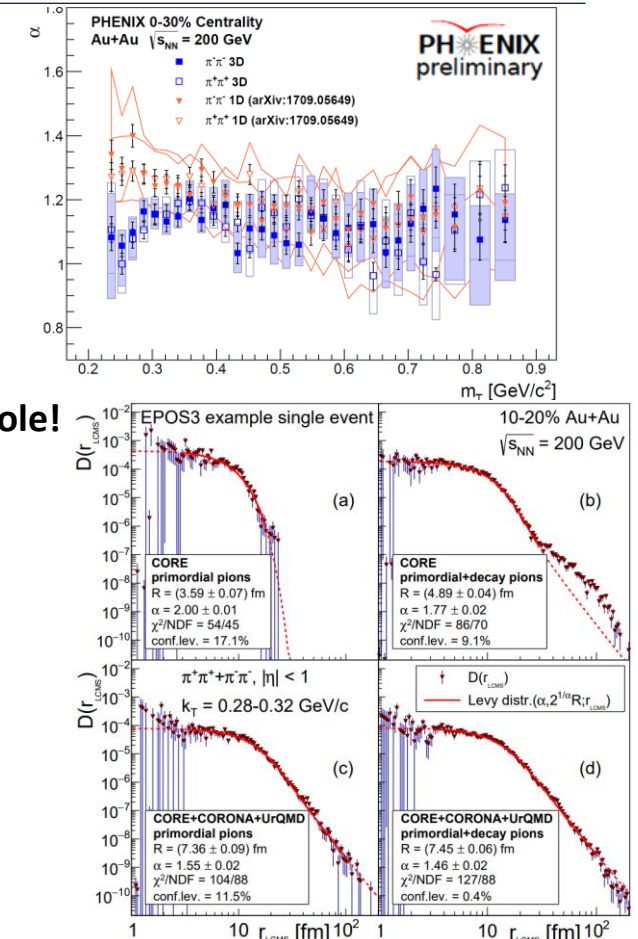
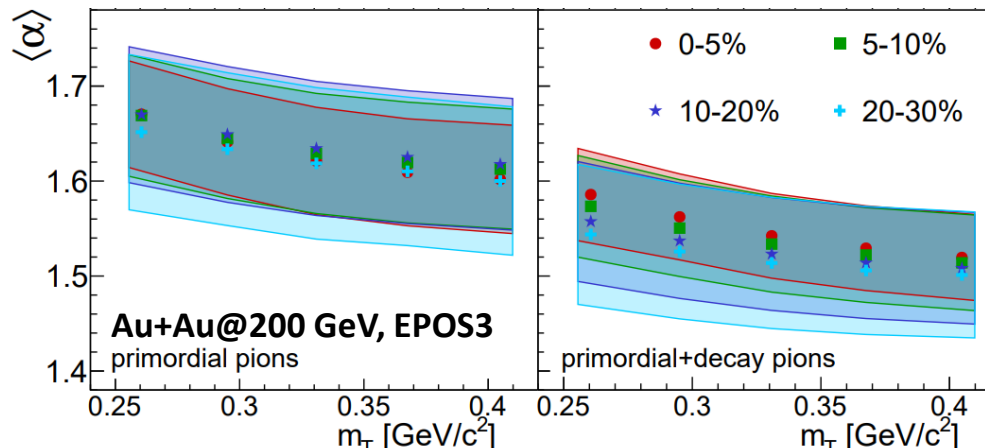
- Not spherically sym. source: 3D vs. 1D α compatible!
 $\alpha < 2$ in 1D analyses not because of angle averaging!

Kurygis, Acta Phys. Pol. B Proc. Suppl. vol. 12 (2), 477 (2019)

$$\mathbf{R}^2 = \begin{pmatrix} R_{out}^2 & 0 & 0 \\ 0 & R_{side}^2 & 0 \\ 0 & 0 & R_{long}^2 \end{pmatrix} \quad \mathbf{q} = \begin{pmatrix} q_{out} \\ q_{side} \\ q_{long} \end{pmatrix}$$

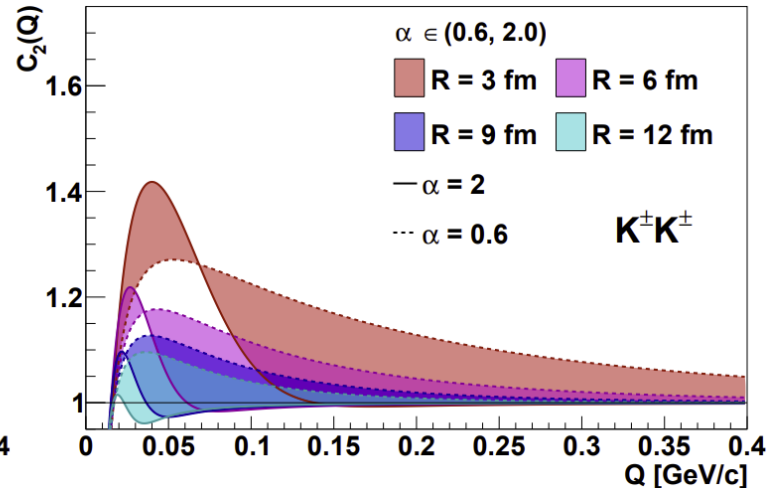
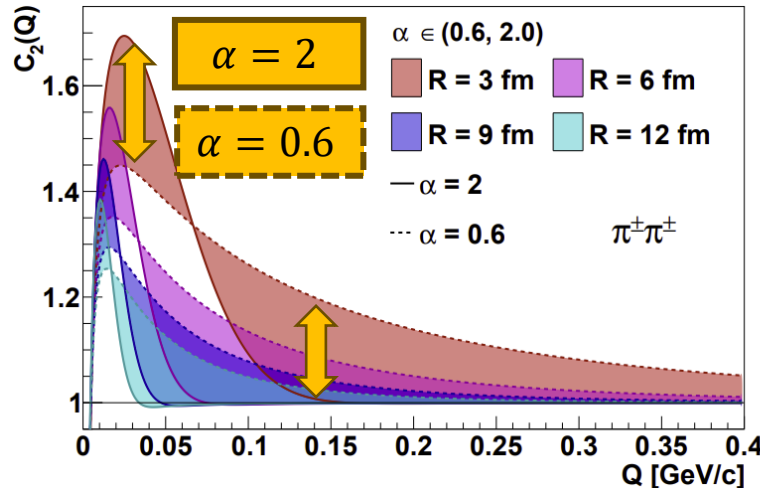
- EPOS pion pair-source analysis at 200 GeV:
Decays and hadronic rescattering (UrQMD) play an important role!

Kincses, Stefaniak, Csanad, Entropy 24 (2022) 3, 308



Recent phenomenological developments

- Coulomb Corrections for Bose-Einstein Correlations from One- and Three-Dimensional Lévy-Type Source Functions *Kurygis, Kincses, Nagy, Csanad, Universe 9 (2023) 7, 328*
- Event-by-Event Investigation of the Two-Particle Source Function in Heavy-Ion Collisions with EPOS *Kincses, Stefaniak, Csanad, Entropy 24 (2022) 3, 308* See talk of M. Csanad!
Korodi, Kincses, Csanad, Phys. Lett. B 847 (2023) 138295
- A novel method for calculating Bose-Einstein correlation functions with Coulomb final-state interaction *Nagy, Purzsa, Csanad, Kincses, Eur. Phys. J. C 83, 1015 (2023)* See talk of M. Nagy!



Part II.

Measurement and fitting of correlation functions



Lévy HBT analysis at STAR, Au+Au @ 200 GeV

- **STAR Run-11 data analyzed**

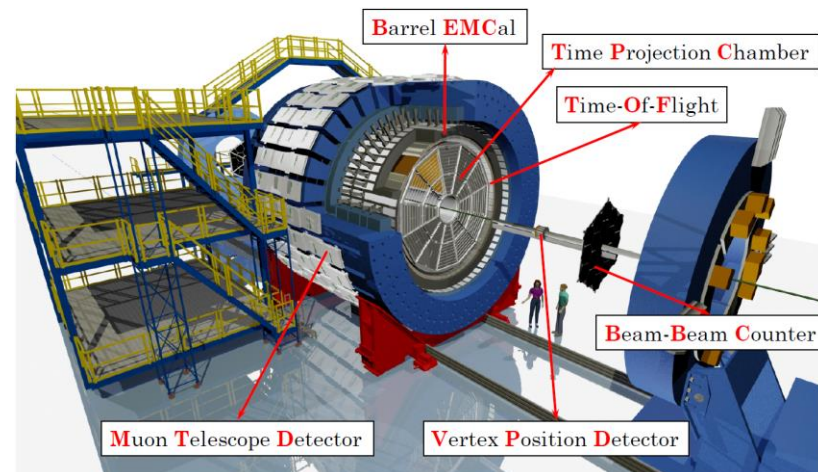
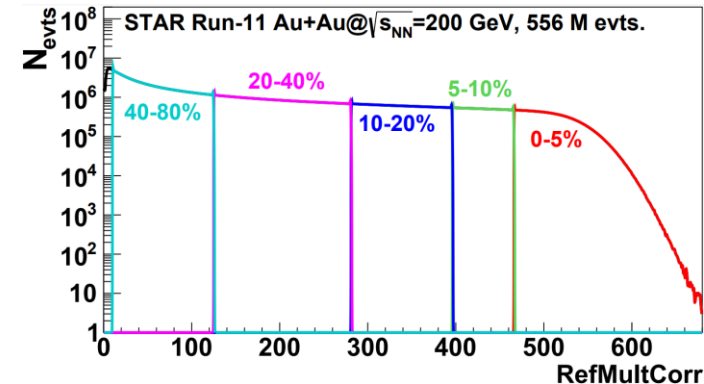
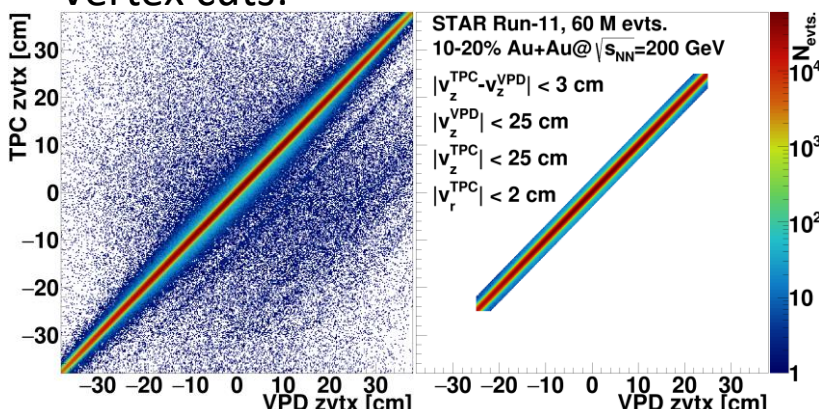
After trigger cuts and bad run cuts: **550M events**

- **Detectors used for the analysis:**

- **BBC, TPC, VPD:** centrality, vertex position
- **TPC:** tracking, dE/dx Particle Identification (PID)
- **TOF:** time-of-flight PID

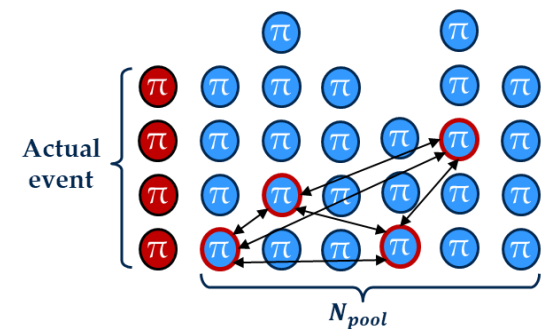
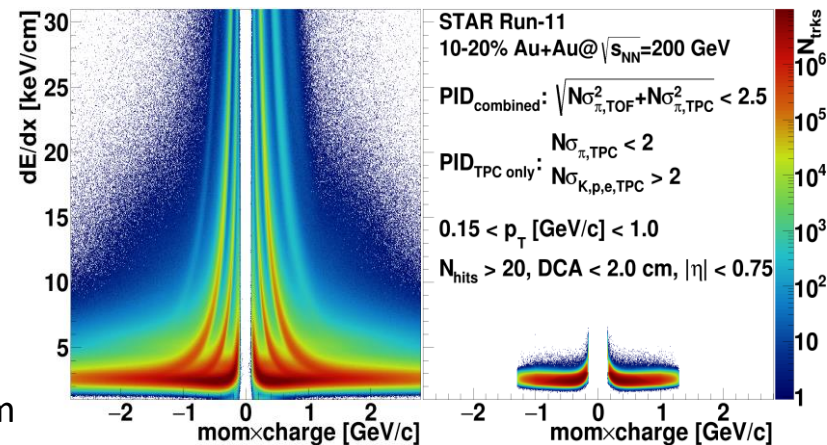
- **Event selection:**

- Pile-up cuts using TOF vs. TPC multiplicity
- Vertex cuts:



Measurement of two-pion correlation functions

- **Track-selection criteria**
 - Combined PID using TPC $N\sigma$ (based on dE/dx) and TOF $N\sigma$ (based on time-of-flight)
 - Further single-track cuts on TPC number of hits, p_T , η , Distance of Closest Approach (DCA)
- **Pair-selection criteria** *J. Adams et al. (STAR Coll.), Phys. Rev. C 71, 044906 (2005)*
 - Splitting level (SL) < 0.6
 - Fraction of Merged Hits (FMH) < 5%
 - Average pair-separation (on TPC pad rows) $\Delta r > 3$ cm
- **Event mixing**
 - Similarly to *PHENIX Coll., Phys. Rev. C 97 (2018) no.6, 064911*
 - 2 cm wide z vertex bins, 5% wide centrality bins
 - A(Q): pions from the same event
 - B(Q): pions from different events
 - C(Q)=A(Q)/B(Q), appropriately normalized
- **Centrality and k_T selection:**
 - 21 k_T bins, (0.175 - 0.750) GeV/c
 - 4 centrality bins (0-10%, 10-20%, 20-30%, 30-40%)



Fitting process with Lévy parametrization

- Lévy parametrization without final state effects:

$$C^{(0)}(Q) = 1 + \lambda \cdot e^{-|RQ|^\alpha}$$

LCMS three-momentum difference

$$Q = |\mathbf{q}_{LCMS}| = \sqrt{(p_{1x} - p_{2x})^2 + (p_{1y} - p_{2y})^2 + q_{long,LCMS}^2}$$

Lévy exponent

Lévy scale parameter

Intercept parameter (correlation strength)

- Formula used for fitting procedure:

$$C(Q) = (1 - \lambda + \lambda \cdot \overbrace{K(Q; \alpha, R)}^{\text{Coulomb correction}} \cdot (1 + e^{-|RQ|^\alpha})) \cdot \overbrace{N \cdot (1 + \varepsilon Q)}^{\text{Possible linear background (usually negligible)}}$$

- Coulomb-correction:

$$K(Q; \alpha, R) = \frac{\int D(r) |\psi^{Coul}(r)|^2 dr}{\int D(r) |\psi^{(0)}(r)|^2 dr}$$

Two-particle wave function (with Coulomb interaction)

Spatial correlations

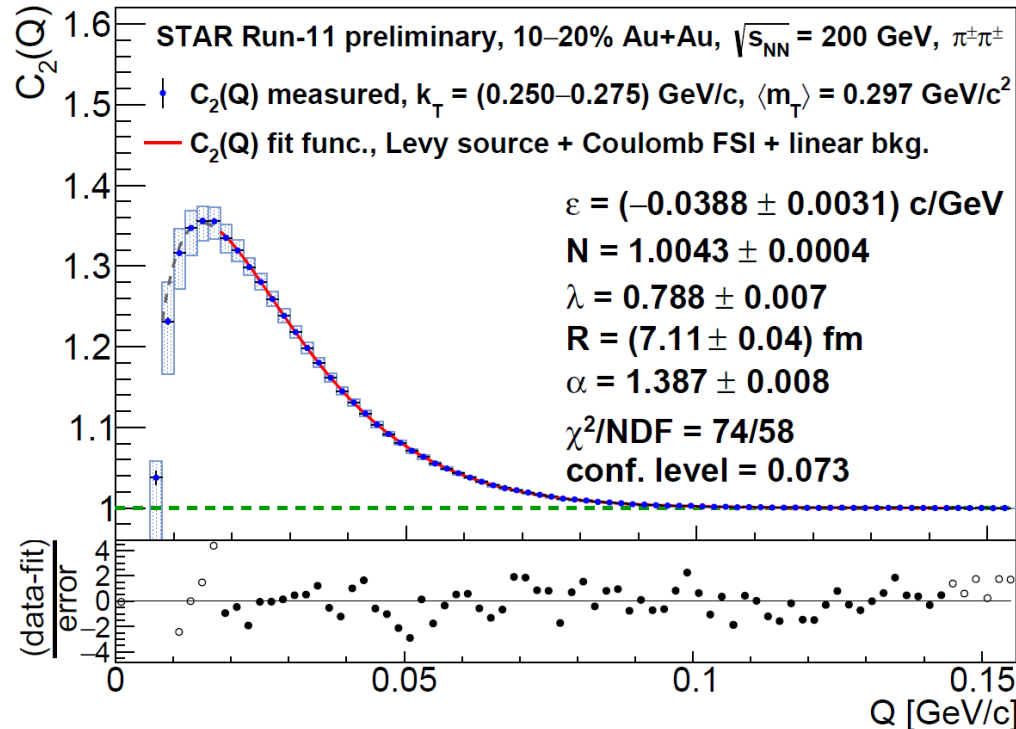
Two-particle wave function (plane wave)

→ calculated numerically
Kincses, Nagy, Csanad, Phys. Rev. C 102 (2020) 6, 064912

$$C(Q) = \left(1 - \lambda + \lambda \cdot K(Q; \alpha, R) \cdot (1 + e^{-|RQ|^{\alpha}})\right) \cdot N \cdot (1 + \varepsilon Q)$$

An example fit to a two-pion correlation function

- Example fit in the 10-20% centrality class, at $k_T = (0.250-0.275)$ GeV/c
- Iterative fitting method,** Coulomb FSI + Lévy-source
- Track and pair syst. uncertainties illustrated with boxes**
- Low-Q points left out from fit, **fit range study included in total systematic uncertainties**
- Fits converged, conf.level > 0.1%**
- Confidence levels approx. uniformly distributed
- Similar fits done in all 4 centrality class and 21 k_T bins, **centrality and m_T dependence of the source parameters investigated**



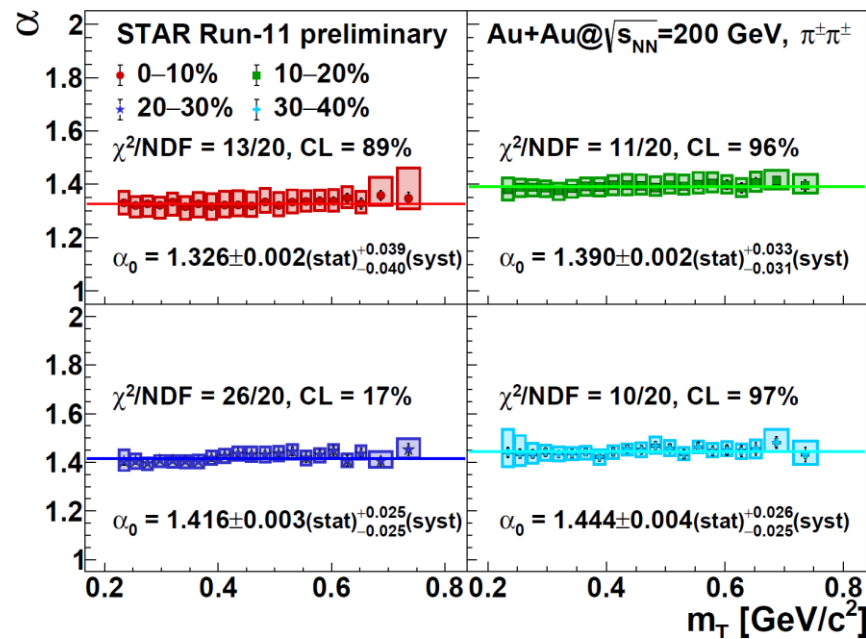
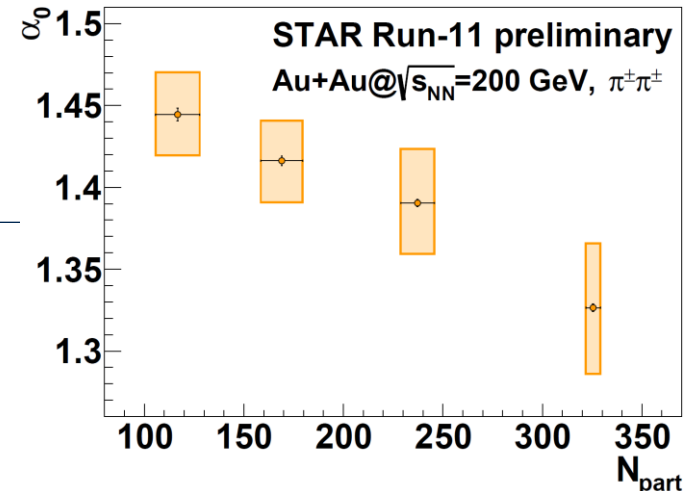
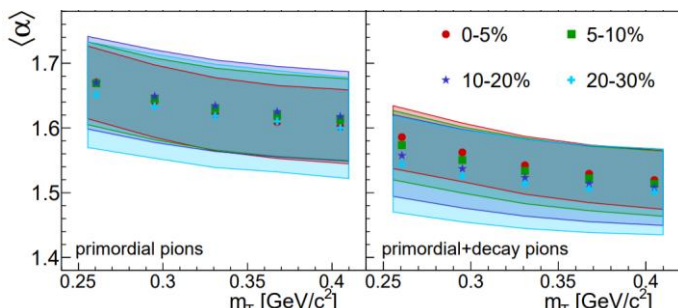
Part III. Preliminary results at 200 GeV (centrality, m_T dependence)



Lévy exponent $\alpha(m_T, \text{centrality})$

- Non-gaussian values ($\alpha \ll 2$)
- No dependence on m_T , slight centrality dep.
- α_0 vs N_{part} (m_T average values from constant fit)
 - Decreasing trend due to anti-correlation with λ and R ?
 - CMS observed opposite trend, see talk of M. Csanad
- EPOS model: slightly higher α values

D. Kincses, M. Stefaniak, M. Csanad, Entropy 24 (2022) 3, 308



Lévy scale $R(m_T, \text{centrality})$

- Decreasing trend with m_T , also with centrality
 - Connection to flow and initial geometry?
- Fits with $R = R_0(A m_T + B)^{-1/\xi}$, $R_0 = 1 \text{ fm}$
 - Hydro calculations (R_{Gauss}): $\xi = 2$

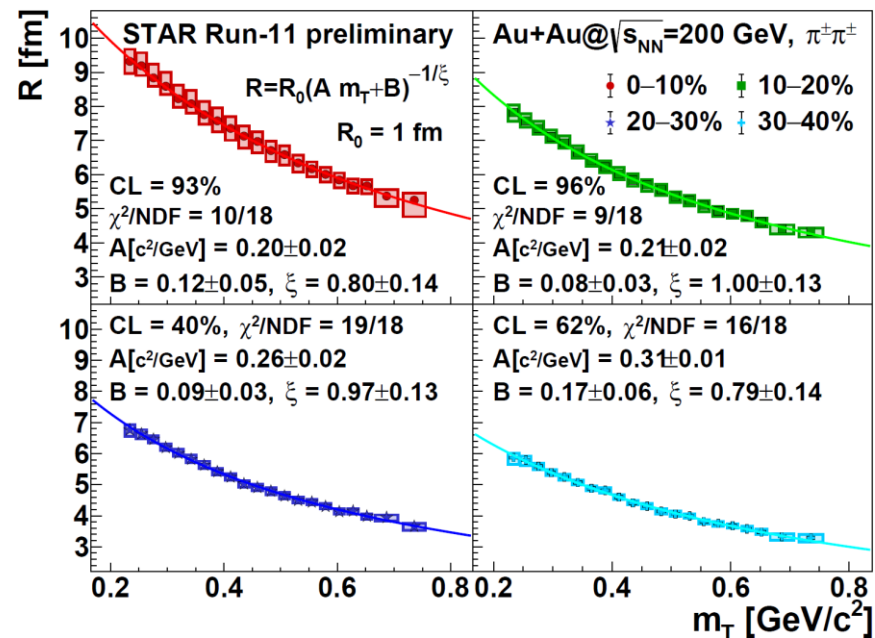
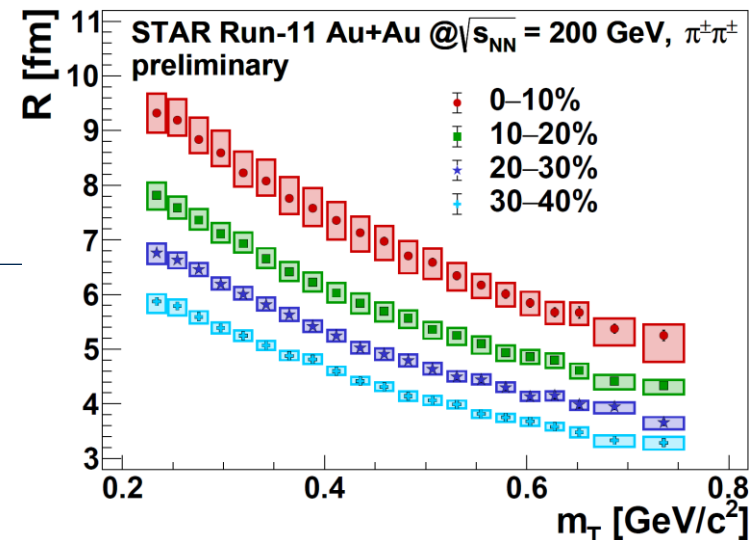
Makhlin, Sinyukov, Z. Phys. C 39, 69 (1988)

Csörgő, Lörstad, Phys. Rev. C 54, 1390 (1996)

Chapman, Scotto, Heinz, Acta Phys. Hung. A 1 (1995) 1-31

Csanád, Csörgő, Lörstad, Ster, J. Phys. G 30, S1079 (2004)

- Our case (R_{Levy}): ξ close to 1



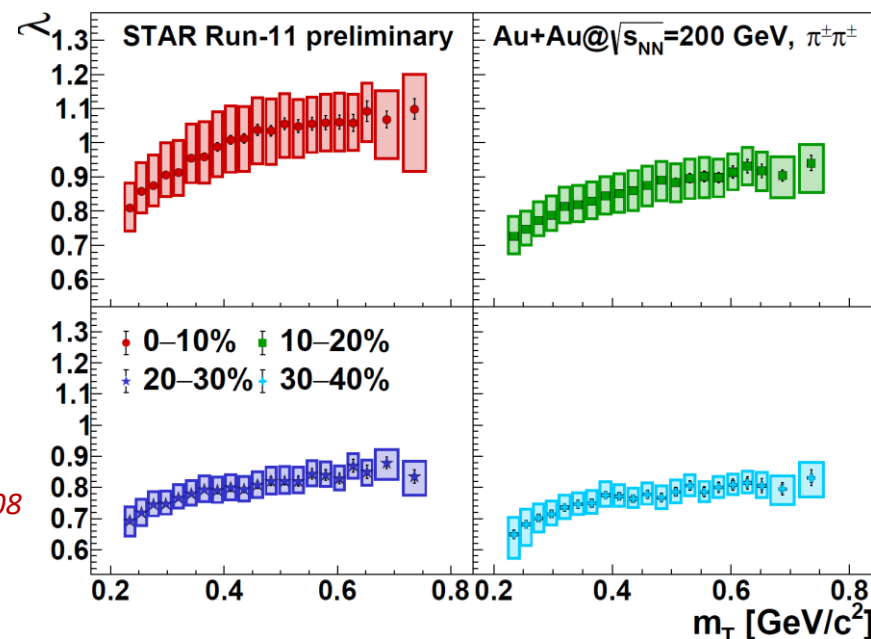
Correlation strength $\lambda(m_T, \text{centrality})$

- Without FSI: $C_2^{(0)}(Q = 0) = 2 \rightarrow \lambda \equiv \lim_{Q \rightarrow 0} C_2^{(0)}(Q) - 1$, experimentally often $\lambda < 1$
- Core-halo picture** - two-component source: $S = S_{\text{core}} + S_{\text{halo}} \Rightarrow D = D_{(c,c)} + D_{(c,h)} + D_{(h,h)}$
 - Core: primordial + decays of short-lived resonances
 - Halo: decays of long-lived resonances \rightarrow large R \rightarrow small Q \rightarrow measurement limited

$$\lambda = N_{\text{core}}^2 / (N_{\text{core}} + N_{\text{halo}})^2$$

*Csörgő, Lörstad, Zimányi, Z.Phys. C71 (1996) 491-497
Bolz et al, Phys.Rev. D47 (1993) 3860-3870;*

- For power-law sources,**
more complicated picture!
- Increase from low to high m_T**
 - More decay products at low m_T ?
 - In-medium mass modification of η' ?
 - Partially coherent particle emission?
- Vance, Csörgő, Kharzeev, Phys. Rev. Lett. 81 (1998), pp. 2205–2208
Bolz et al., Phys. Rev. D47 (1993), pp. 3860–3870*
- Decrease from central to peripheral**

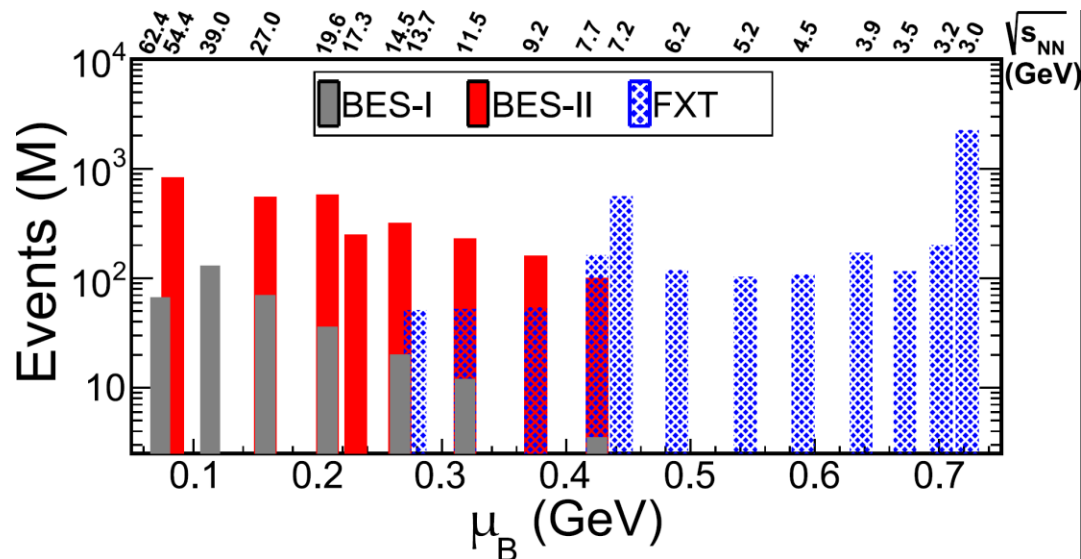


Part IV. Preliminary results at BES-II $(\sqrt{s_{NN}}, m_T$ dependence)



Beam energy dependent analysis in Au+Au collisions

- **BES-II data taking** recently conducted at STAR
 - Increased luminosity
 - Many detector improvements
- Next step: similar analysis with the same settings at lower Au+Au energies
 - Run-17, **54.4 GeV**
 - Run-18, **27 GeV**
 - Run-19, **19.6 GeV**
 - Run-19, **14.5 GeV**
 - Run-21, **7.7 GeV**



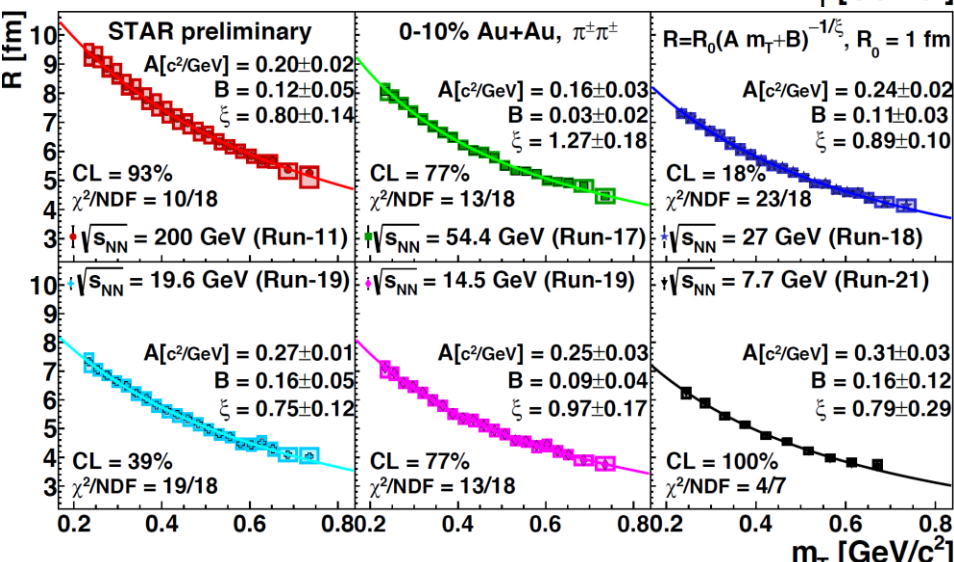
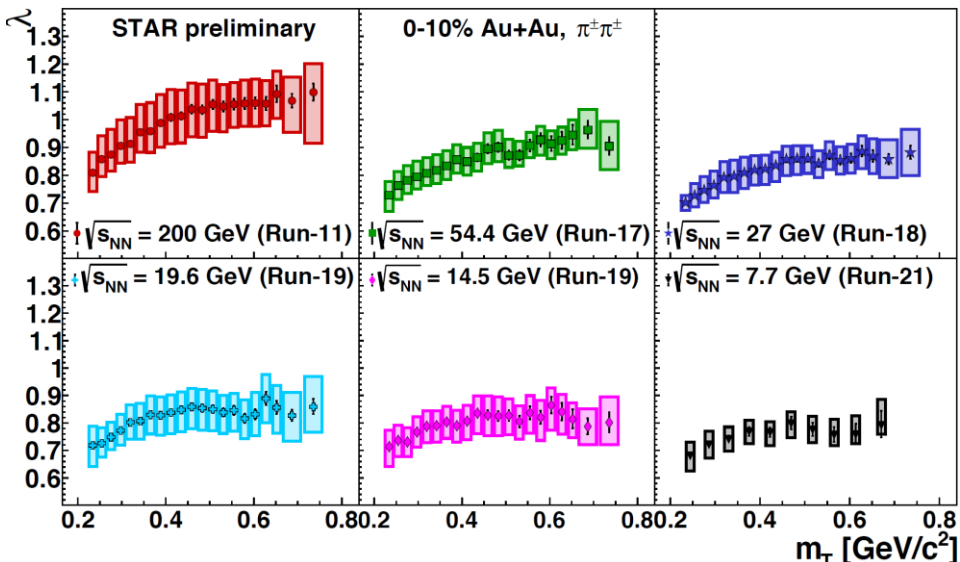
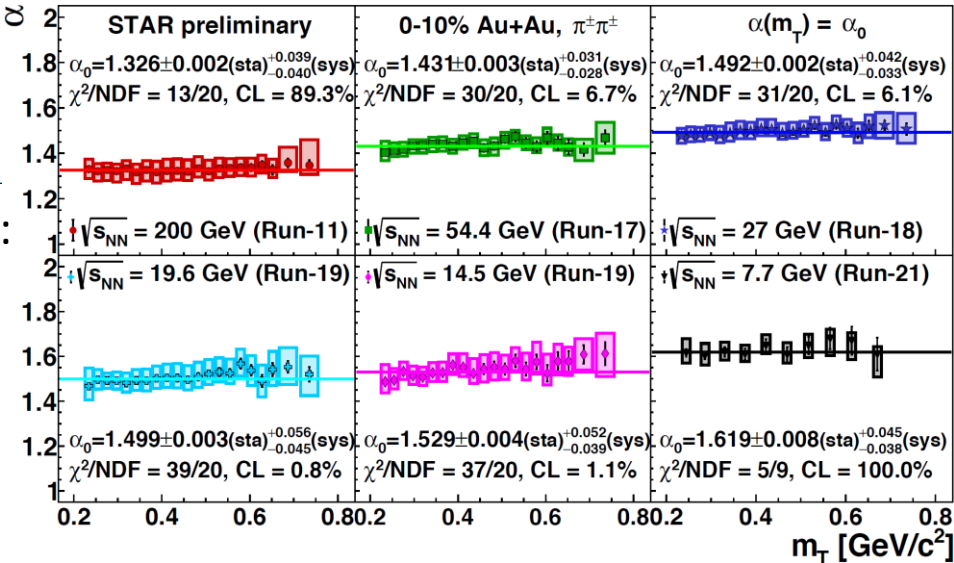
$\sqrt{s_{NN}}$ and m_T dependence of the source parameters

- $\sqrt{s_{NN}}$ dependence from 200 to 7.7 GeV:

$$\alpha \uparrow, R \downarrow, \lambda \downarrow$$

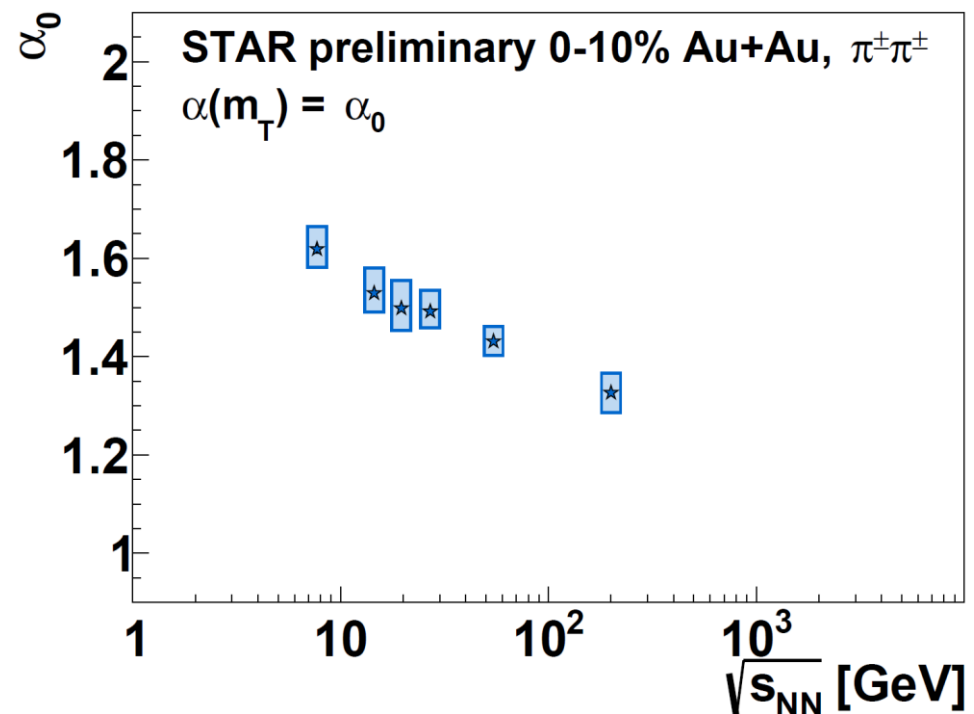
- m_T dependent trends at all energies:

$$\alpha \text{ const.}, R \downarrow, \lambda \uparrow$$



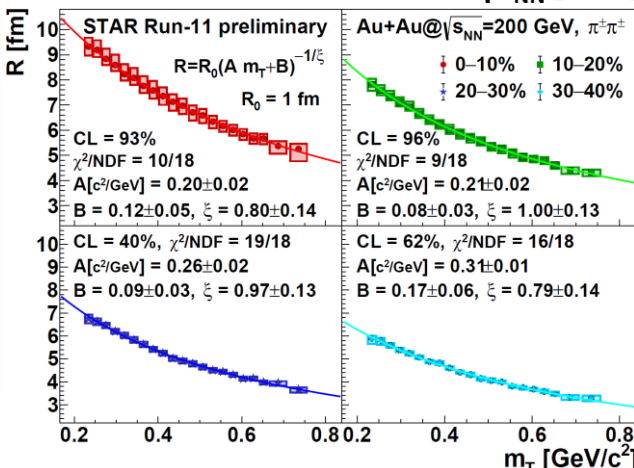
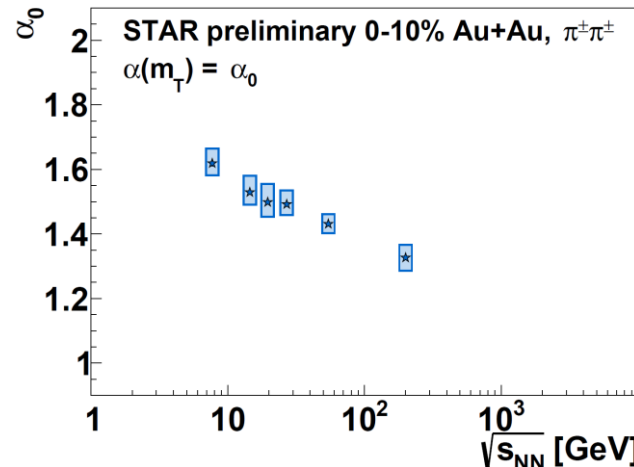
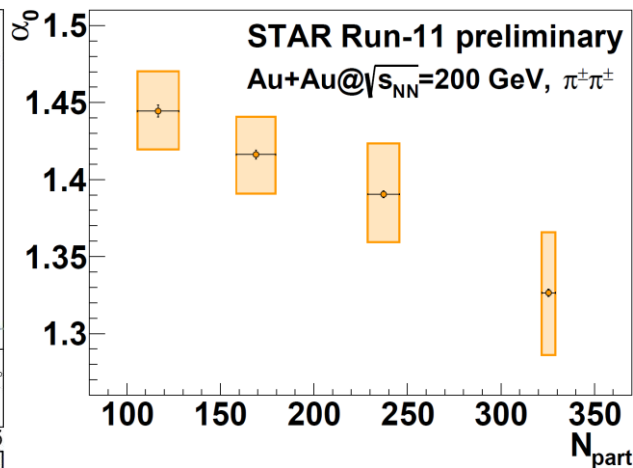
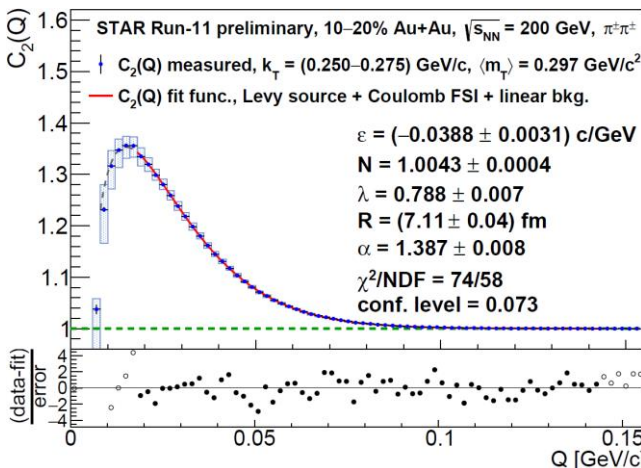
Excitation function of the Lévy exponent

- Non-gaussian values ($\alpha \ll 2$)
- Monotonic decrease from 7.7 GeV to 200 GeV
- CMS 0-10% PbPb result at 5.02 TeV:
arXiv:2306.11574 $\alpha_0 \approx 1.86$
(note that the kinematic range is different, see talk of M. Csanad)
- Interpretation of α still an open question, possibilities include:
 - Jet fragmentation
 - Critical behavior
 - Event averaging
 - Resonance decays
 - Anomalous diffusion



Summary

- 1-dim. two-pion correlation functions investigated
- Lévy-source + Coulomb FSI → good description
- Further syst. uncertainty investigations underway
- 0-10% Au+Au: **200 GeV** → **7.7 GeV** $\alpha \uparrow, R \downarrow, \lambda \downarrow$
200 GeV Au+Au: **central** → **peripheral**
- Next steps: even lower energies (fxt), 3D analysis!



Further details, backup slides



Systematic uncertainties

- **Systematic uncertainties already investigated:**
 - Single track- and pair-cut variations, fit limits
- **Systematic uncertainties to be investigated:**
 - Purity correction, momentum smearing, more detailed fit limit study, strong interaction

TABLE II. Sources of systematic uncertainties.

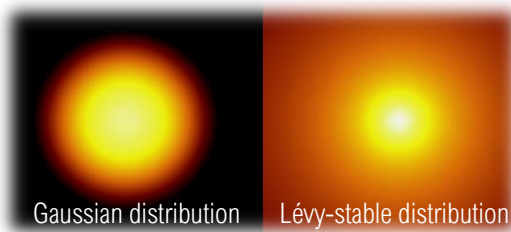
<i>n</i>	source of uncertainty	settings (<i>j</i> = 0, 1, ...)
0	NHitsFit cut	18, 20, 22
1	DCA cut	1.5 cm, 2 cm, 2.5 cm
2	$ \eta $ cut	0.5, 0.75, 1.0
3	PID $N\sigma$	default, loose, strict
4	SL cut	0.5, 0.6, 0.7
5	FMH cut	0%, 5%, 10%
6	$\Delta u, \Delta z$ limits	default, loose, strict
7	Lower fit limit in Q	default, +1 bin, -1 bin
8	Higher fit limit in Q	default, +5 bin, -5 bin

TABLE III. m_T averaged asymmetric systematic uncertainties [%].

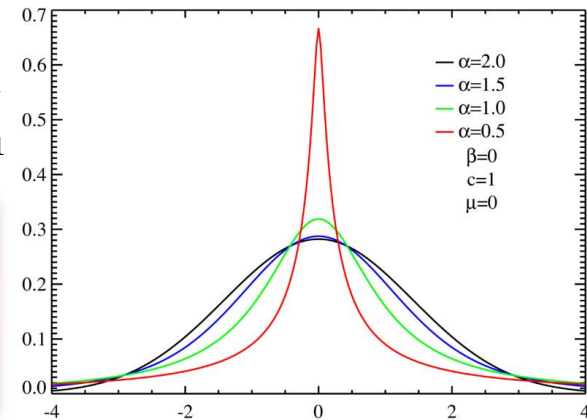
<i>n</i>	source of uncertainty	settings (<i>j</i> = 0, 1, ...)	λ						R						α					
			0–10%	10–20%	20–30%	30–40%	0–10%	10–20%	20–30%	30–40%	0–10%	10–20%	20–30%	30–40%	0–10%	10–20%	20–30%	30–40%		
0	NHitsFit cut	18, 20, 22	n	$\langle \delta \uparrow \rangle$	$\langle \delta \downarrow \rangle$	$\langle \delta \uparrow \rangle$	$\langle \delta \downarrow \rangle$	$\langle \delta \uparrow \rangle$	$\langle \delta \downarrow \rangle$	$\langle \delta \uparrow \rangle$	$\langle \delta \downarrow \rangle$	$\langle \delta \uparrow \rangle$	$\langle \delta \downarrow \rangle$	$\langle \delta \uparrow \rangle$	$\langle \delta \downarrow \rangle$	$\langle \delta \uparrow \rangle$	$\langle \delta \downarrow \rangle$	$\langle \delta \uparrow \rangle$	$\langle \delta \downarrow \rangle$	
1	DCA cut	1.5 cm, 2 cm, 2.5 cm	0	3.4	2.1	1.6	1.1	0.7	0.5	0.3	0.2	1.4	0.9	0.7	0.5	0.3	0.2	0.2	0.1	0.2
2	$ \eta $ cut	0.5, 0.75, 1.0	1	4.2	2.9	3.6	2.6	3.3	2.5	3.0	2.2	0.7	0.4	0.4	0.3	0.3	0.3	0.2	0.2	0.2
3	PID $N\sigma$	default, loose, strict	2	1.2	1.1	0.4	0.6	0.7	0.8	0.6	1.5	0.6	0.7	0.2	0.4	0.4	0.5	0.3	0.9	0.7
4	SL cut	0.5, 0.6, 0.7	3	1.3	0.4	1.3	0.6	1.3	0.6	1.7	1.0	0.7	0.3	0.6	0.3	0.6	0.4	0.8	0.6	0.8
5	FMH cut	0%, 5%, 10%	4	0.2	0.1	0.1	0.0	0.1	0.0	0.0	0.0	0.1	0.0	0.1	0.0	0.0	0.0	0.0	0.0	0.0
6	$\Delta u, \Delta z$ limits	default, loose, strict	5	5.4	6.0	4.0	4.4	3.0	3.1	2.5	2.8	2.6	3.1	2.0	2.2	1.5	1.5	1.2	1.3	2.5
7	Lower fit limit in Q	default, +1 bin, -1 bin	6	3.5	4.2	2.5	3.0	1.9	2.1	1.7	1.9	1.7	2.1	1.3	1.5	0.9	1.0	0.8	0.9	1.7
8	Higher fit limit in Q	default, +5 bin, -5 bin	7	0.5	0.5	0.7	0.7	0.5	0.4	0.9	0.6	0.3	0.3	0.4	0.4	0.3	0.2	0.5	0.4	0.6
			8	1.4	1.1	0.7	0.8	0.7	0.8	1.1	1.2	0.8	0.6	0.4	0.5	0.3	0.4	0.3	0.3	0.7
			Σ	8.7	8.3	6.4	6.2	5.2	4.7	4.9	4.6	3.7	4.0	2.6	2.8	2.0	2.0	1.8	1.9	3.3

Properties of univariate stable distributions

- **Univariate stable distribution:** $f(x) = \frac{1}{2\pi} \int_{-\infty}^{\infty} \varphi(q) e^{-ixq} dq$, where the characteristic function:
- $\varphi(q; \alpha, \beta, R, \mu) = \exp(iq\mu - |qR|^\alpha(1 - i\beta \operatorname{sgn}(q)\Phi))$
- α : index of stability
- β : skewness, symmetric if $\beta = 0$
- R : scale parameter
- μ : location, equals the median,
if $\alpha > 1$: μ = mean



$$\Phi = \begin{cases} \tan\left(\frac{\pi\alpha}{2}\right), & \alpha \neq 1 \\ -\frac{2}{\pi} \log|q|, & \alpha = 1 \end{cases}$$



In 3D: $\mathcal{L}(r; \alpha, R) = \frac{1}{(2\pi)^3} \int d^3q e^{iqr} e^{-\frac{1}{2}|qRq|^{\alpha}/2}$

- **Important characteristics of stable distributions:**

- Retains same α and β under convolution of random variables
- Any moment greater than α isn't defined

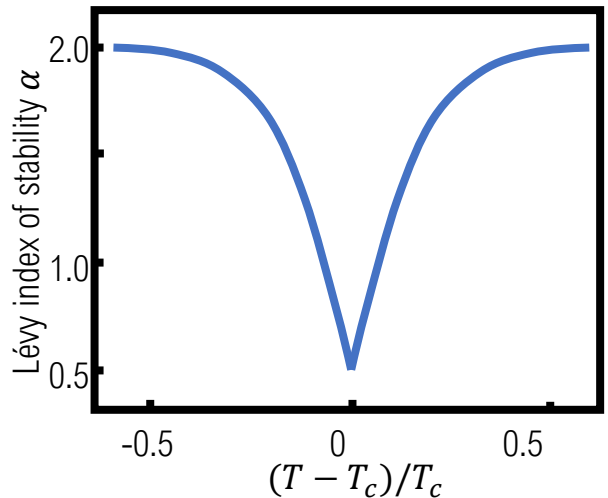
$$R_{\sigma\nu}^2 = \begin{pmatrix} 0 & 0 & 0 & 0 \\ 0 & R_{\text{out}}^2 & 0 & 0 \\ 0 & 0 & R_{\text{side}}^2 & 0 \\ 0 & 0 & 0 & R_{\text{long}}^2 \end{pmatrix}$$

Second order phase transition?

- Second order phase transitions: **critical exponents**
 - **Near the critical point**
 - Specific heat $\sim ((T - T_c)/T_c)^{-\alpha}$
 - Order parameter $\sim ((T - T_c)/T_c)^{-\beta}$
 - Susceptibility/compressibility $\sim ((T - T_c)/T_c)^{-\gamma}$
 - Correlation length $\sim ((T - T_c)/T_c)^{-\nu}$
 - **At the critical point**
 - Order parameter $\sim (\text{source field})^{1/\delta}$
 - **Spatial correlation function** $\sim r^{-d+2-\eta}$
- Ginzburg-Landau: $\alpha = 0, \beta = 0.5, \gamma = 1, \eta = 0.5, \delta = 3, \eta = 0$
- QCD \leftrightarrow 3D Ising model
- Can we measure the η power-law exponent?
- Depends on spatial distribution: measurable with femtoscopy!
- **What distribution has a power-law exponent? Levy-stable distribution!**

Lévy index as critical exponent?

- Critical spatial correlation: $\sim r^{-(d-2+\eta)}$;
Lévy source: $\sim r^{-(1+\alpha)}$; $\alpha \Leftrightarrow \eta$?
Csörgő, Hegyi, Zajc, Eur.Phys.J. C36 (2004) 67
- QCD universality class \leftrightarrow 3D Ising
Halasz et al., Phys.Rev.D58 (1998) 096007
Stephanov et al., Phys.Rev.Lett.81 (1998) 4816
- At the critical point:
 - Random field 3D Ising: $\eta = 0.50 \pm 0.05$
Rieger, Phys.Rev.B52 (1995) 6659
 - 3D Ising: $\eta = 0.03631(3)$
El-Showk et al., J.Stat.Phys.157 (4-5): 869
- Motivation for precise Lévy HBT!
- **Change in α_{Levy} - proximity of CEP?**



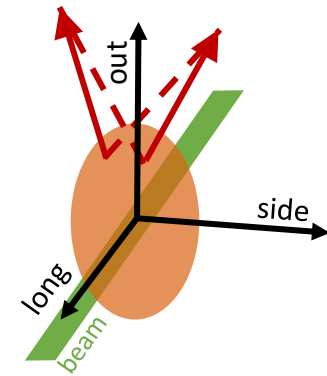
- Modulo finite size/time and non-equilibrium effects
- Other possible reasons for Lévy distributions: anomalous diffusion, QCD jets, ...

Kinematic variables of the correlation function I.

- Smoothness approximation ($p_1 \approx p_2 \approx K$): $S(x_1, K - q/2) S(x_2, K + q/2) \approx S(x_1, K) S(x_2, K)$
- $C_2(q, K) = \int d^4r D(r, K) \left| \psi_q^{(2)}(\mathbf{r}) \right|^2$
- Without any FSI $\left| \psi_q^{(2)}(\mathbf{r}) \right|^2 = 1 + \cos(q\mathbf{r})$
- **HBT correlation function in direct connection with Fourier transform of the pair-source function**
- Important to determine the nature and dimensionality of the correlation function
- Lorentz-product of $q = (q_0, \mathbf{q})$ and $K = (K_0, \mathbf{K})$ is zero, i.e.: $qK = q_0 K_0 - \mathbf{q}\mathbf{K} = 0$
- Energy component of q can be expressed as $q_0 = \mathbf{q} \frac{\mathbf{K}}{K_0}$
- If the energy of the particles are similar, K is approximately on shell
- **Correlation function can be measured as a function of three-momentum variables**

Kinematic variables of the correlation function II.

- $C_2(\mathbf{q}, \mathbf{K})$ as a function of three-momentum variables
- \mathbf{K} dependence is smoother, \mathbf{q} is the main kinematic variable
- Close to mid-rapidity one can use $k_T = \sqrt{K_x^2 + K_y^2}$, or $m_T = \sqrt{k_T^2 + m^2}$
- For any fixed value of m_T , the correlation function can be measured as a function of \mathbf{q} only
- Usual decomposition: **out-side-long or Bertsch-Pratt (BP) coordinate-system**
 - $\mathbf{q} \equiv (q_{out}, q_{side}, q_{long})$
 - long: beam direction
 - out: k_T direction
 - side: orthogonal to the others
 - Essentially a rotation in the transverse plane
- Customary to use a Lorentz-boost in the long direction and change to the **Longitudinal Co-Moving System (LCMS)** where the average longitudinal momentum of the pair is zero



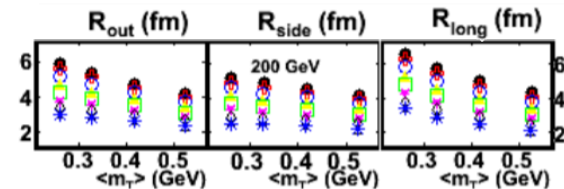
Kinematic variables of the correlation function III.

- Drawback of a 3D measurement: lack of statistics, difficulties of a precise shape analysis
- **What is the appropriate one-dimensional variable?**
- Lorentz-invariant relative momentum: $q_{inv} \equiv \sqrt{-q^\mu q_\mu} = \sqrt{q_x^2 + q_y^2 + q_z^2 - (E_1 - E_2)^2}$
- Equivalent to three-mom. diff. in Pair Co-Moving System (PCMS), where $E_1 = E_2$: $q_{inv} = |\mathbf{q}_{PCMS}|$
- In LCMS using BP variables: $q_{inv} = \sqrt{(1 - \beta_T)^2 q_{out}^2 + q_{side}^2 + q_{long}^2}$ $\beta_T = 2k_T/(E_1 + E_2)$
- **Value of q_{inv} can be relatively small even when q_{out} is large!**
- Experimental indications: **in LCMS source is \approx spherically symmetric**
- Correlation function boosted to PCMS will not be spherically symmetric
- Let us introduce the following variable invariant to Lorentz boosts in the beam direction:

$$Q \equiv |\mathbf{q}_{LCMS}| = \sqrt{(p_{1x} - p_{2x})^2 + (p_{1y} - p_{2y})^2 + q_{z,LCMS}^2}$$

$$\text{where } q_{z,LCMS}^2 = \frac{4(p_{1z}E_2 - p_{2z}E_1)^2}{(E_1 + E_2)^2 - (p_{1z} + p_{2z})^2}.$$

STAR, Phys.Rev.C 92 (2015) 1, 014904



Kinematic variables of the correlation function IV.

- Nature of the 1D variable in experiment: check correlation function in two dimensions!

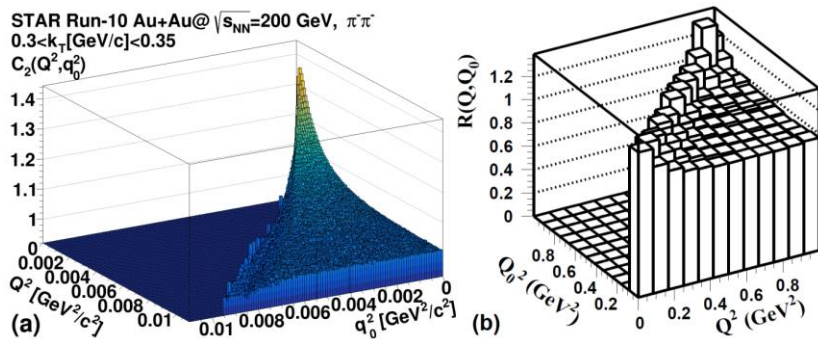


Figure 3.4: Example two-dimensional pion correlation functions for $\sqrt{s_{NN}} = 200$ GeV Au+Au collisions (a) and $\sqrt{s} = 91$ GeV e^+e^- collisions (b). The latter figure is taken from the thesis of Tamás Novák [161].

Q dep. corr.func.

q_{inv} dep. corr.func.

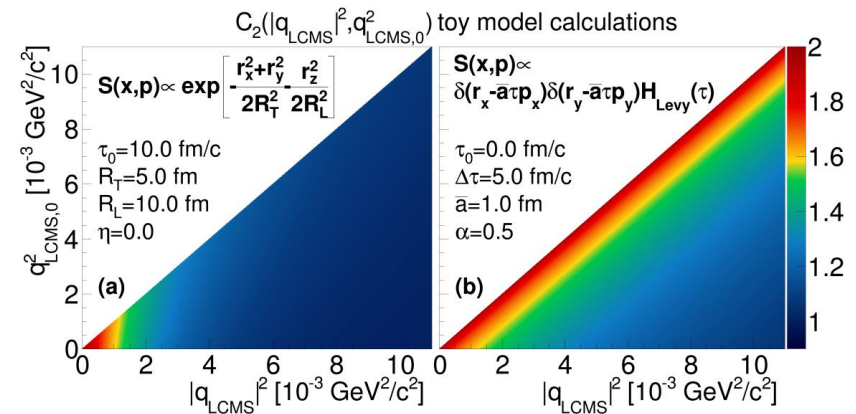
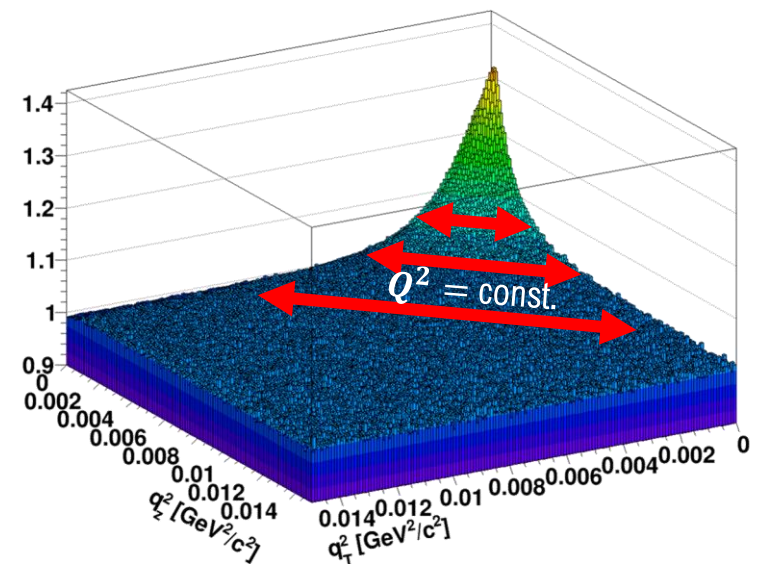
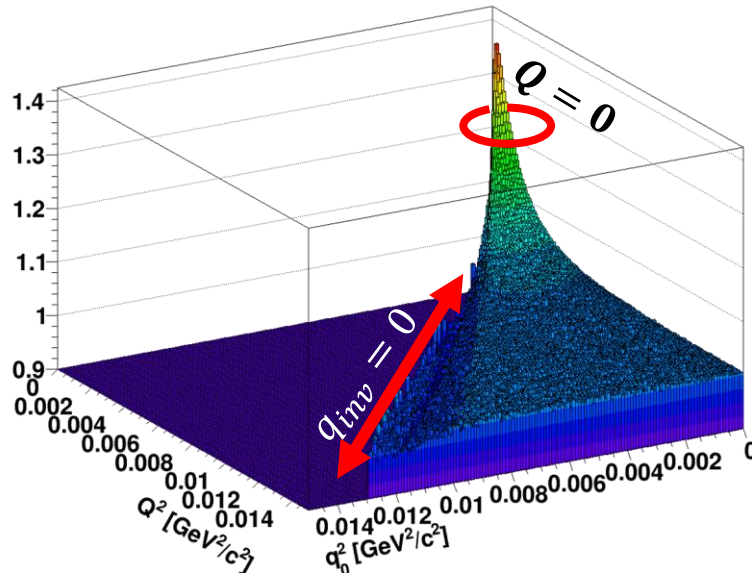


Figure 3.5: Toy model calculation for two different types of source functions. Taking a Gaussian source in both space and time leads to a correlation function that depends mostly on $|q_{LCMS}|$ (a), while a source that shows strong space-time and momentum space correlation leads to a q_{inv} dependent correlation function (b).

Kinematic variables of the correlation function V.

- Nature of the 1D variable in experiment: check correlation function in two dimensions!

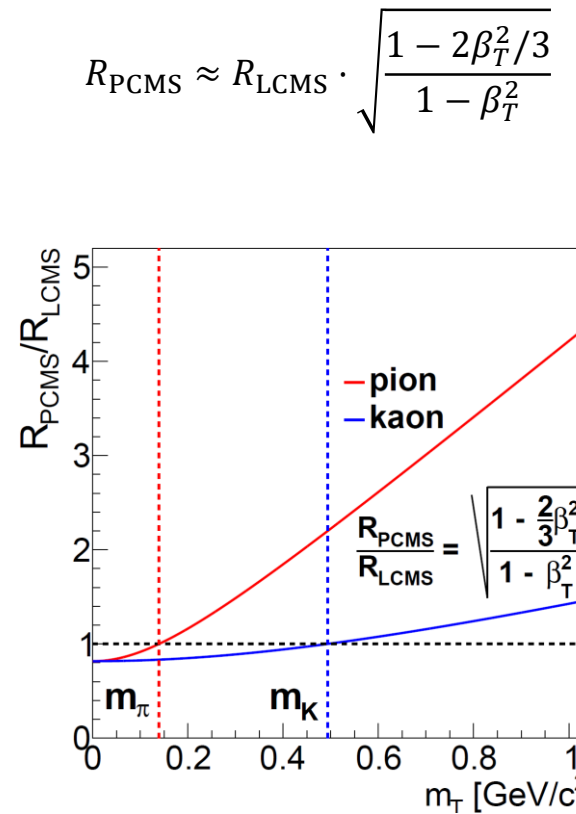
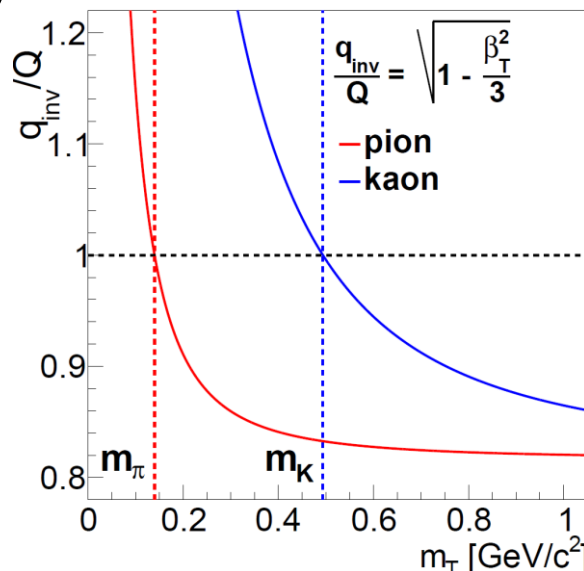
$$Q = |\mathbf{q}_{LCMS}| = \sqrt{(p_{1x} - p_{2x})^2 + (p_{1y} - p_{2y})^2 + q_{long,LCMS}^2}$$



D. Kincses, Ph.D. thesis, [10.15476/ELTE.2022.164](https://doi.org/10.15476/ELTE.2022.164)

Kinematic variables of the correlation function VI.

- Correlation function measured in LCMS, Coulomb effect calculated in PCMS
- Approximation:
$$q_{\text{inv}} \equiv q_{\text{PCMS}} \approx q_{\text{LCMS}} \cdot \sqrt{1 - \beta_T^2/3}$$
$$R_{\text{PCMS}} \approx R_{\text{LCMS}} \cdot \sqrt{\frac{1 - 2\beta_T^2/3}{1 - \beta_T^2}}$$
- (Note $m_T < m$
not physical of course)



Coulomb correction and fitting of the corr. function

- Core-Halo model, Bowler-Sinyukov method: $C_2(Q, k_T) = 1 - \lambda + \lambda \int d^3\mathbf{r} D_{(c,c)}(\mathbf{r}, k_T) |\Psi_Q^{(2)}(\mathbf{r})|^2$
- Neglecting FSI and using a Lévy-stable source function: $C_2^{(0)}(Q, k_T) = 1 + \lambda e^{-|RQ|^\alpha}$
- **Using numerical integral calculation as fit function results in numerically fluctuating χ^2 landscape**
- Treat FSI as correction factor: $K(Q, k_T) = \frac{C_2(Q, k_T)}{C_2^{(0)}(Q, k_T)}$
- An iterative method can be used: $C_2^{(fit)}(Q; \lambda, R, \alpha) = C_2^{(0)}(Q; \lambda, R, \alpha) \cdot K(Q; \lambda_0, R_0, \alpha_0)$
- Procedure continued until $\Delta_{\text{iteration}} = \sqrt{\frac{(\lambda_{n+1}-\lambda_n)^2}{\lambda_n^2} + \frac{(R_{n+1}-R_n)^2}{R_n^2} + \frac{(\alpha_{n+1}-\alpha_n)^2}{\alpha_n^2}} < 0.01$
- **Iterations usually converge within 2-3 rounds, fit parameters can be reliably extracted**

Coulomb correction and fitting of the corr. function

- Lévy-type correlation function without final state effects: $C^{(0)}(Q) = 1 + \lambda \cdot e^{-|RQ|^\alpha}$
- Bowler-Sinyukov method:

$$C(Q_{LCMS}; \lambda, R_{LCMS}, \alpha) = (1 - \lambda + \lambda \cdot K(q_{inv}; \alpha, R_{PCMS}) \cdot (1 + e^{-|R_{LCMS}Q_{LCMS}|^\alpha})) \cdot N \cdot (1 + \varepsilon Q_{LCMS})$$

↑
Intercept parameter
(correlation strength)
↓
Coulomb correction

↑
Lévy scale parameter
↓
Lévy exponent

Possible linear
background
(usually negligible)

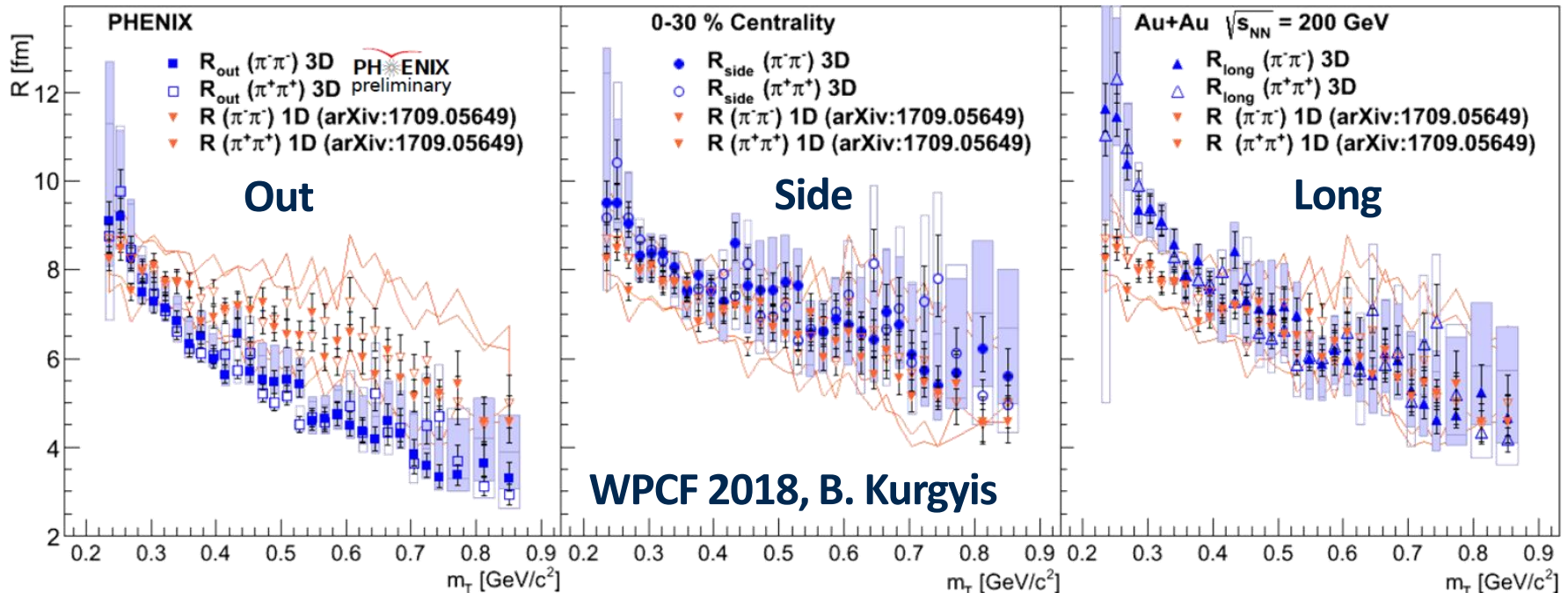
- Coulomb-correction calculated numerically (in PCMS)

$$q_{inv} \equiv q_{PCMS} \approx q_{LCMS} \cdot \sqrt{1 - \beta_T^2/3}$$

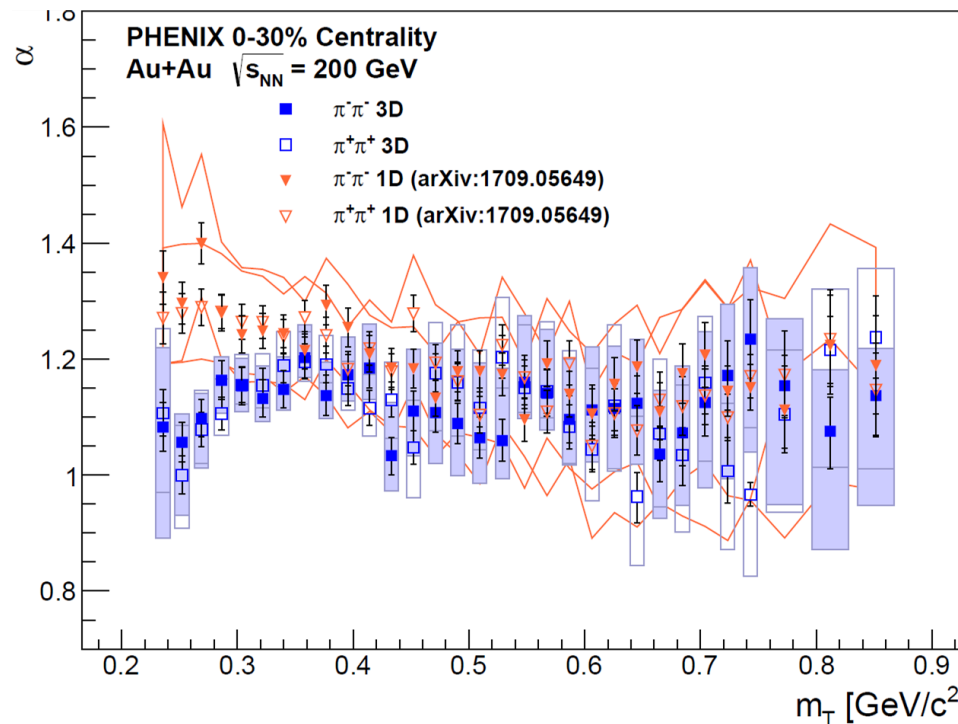
$$R_{PCMS} \approx R_{LCMS} \cdot \sqrt{\frac{1 - 2\beta_T^2/3}{1 - \beta_T^2}}$$

Cross-check with 3D analysis – PHENIX preliminary

$$C(Q) = \left(1 - \lambda + \lambda \cdot K(q_{inv}; \alpha, R_{inv}) \cdot (1 + e^{-|R_o^2 q_o^2 + R_s^2 q_s^2 + R_l^2 q_l^2|^{\alpha/2}}) \right) \cdot N \cdot (1 + \varepsilon Q)$$



Cross-check with 3D analysis – PHENIX preliminary



- **Compatible with 1D (Q_{LCMS}) measurement** of Phys. Rev. C 97, 064911 (2018)
- Small discrepancy at small m_T : due to large R_{long} at small m_T ?

3D Gaussian vs 1D Levy

- **3D Gaussian does not result in 1D Levy**
 - Difference: several percent
 - Available experimental precision: much better than this difference

